

Full-sky interferometry

Simulating full-sky interferometric observations

Jason McEwen

<http://www.mrao.cam.ac.uk/~jdm57/>

Anna Scaife

<http://www.mrao.cam.ac.uk/people/ascaife.html>

**Astrophysics Group, Cavendish Laboratory
University of Cambridge**

<http://arxiv.org/abs/0803.2165>

Motivation (and disclaimer)

- Aperture array interferometers, such as that proposed for the SKA, will see a large portion of the sky.
- Usual Fourier transform approach for simulating visibilities relies on a tangent plane approximation that is only valid for small fields of view.
- We address the **forward wide field imaging problem** and consider full-sky contributions to the visibilities observed by an interferometer, ensuring that contamination due to wide sidelobes of the primary beam is not neglected.
- Disclaimer
- Outline of talk
 - Harmonic analysis
 - Coordinate systems
 - Computing visibilities (and image reconstruction)
 - Preliminary simulations
 - Fast wavelet methods

Spherical harmonics

- A square integrable function on the sphere $F \in L^2(S^2, d\Omega)$ may be represented by the **spherical harmonic expansion**

$$F(\hat{s}) = \sum_{\ell=0}^{\infty} \sum_{m=-\ell}^{\ell} F_{\ell m} Y_{\ell m}(\hat{s}) .$$

- The **spherical harmonic coefficients** are given by the usual projection onto the spherical harmonic basis functions:

$$F_{\ell m} = \int_{S^2} F(\hat{s}) Y_{\ell m}^*(\hat{s}) d\Omega(\hat{s}) ,$$

where $d\Omega(\hat{s}) = \sin \theta d\theta d\varphi$ is the usual rotation invariant measure on the sphere and $\hat{s} = (\theta, \varphi) \in S^2$ denote spherical coordinates with colatitude $\theta \in [0, \pi]$ and longitude $\varphi \in [0, 2\pi)$.

- Useful **properties and relations**
 - Orthogonality

$$\int_{S^2} Y_{\ell m}(\hat{s}) Y_{\ell' m'}^*(\hat{s}) d\Omega(\hat{s}) = \delta_{\ell\ell'} \delta_{mm'}$$

- Addition theorem

$$\sum_{m=-\ell}^{\ell} Y_{\ell m}(\hat{s}) Y_{\ell m}^*(\hat{s}') = \frac{2\ell+1}{4\pi} P_{\ell}(\hat{s} \cdot \hat{s}')$$

- Jacobi-Anger expansion

$$e^{i\mathbf{x} \cdot \mathbf{y}} = \sum_{\ell=0}^{\infty} (2\ell+1) i^{\ell} j_{\ell}(\|\mathbf{x}\| \|\mathbf{y}\|) P_{\ell}(\hat{\mathbf{x}} \cdot \hat{\mathbf{y}})$$

Spherical harmonics

- A square integrable function on the sphere $F \in L^2(S^2, d\Omega)$ may be represented by the **spherical harmonic expansion**

$$F(\hat{\mathbf{s}}) = \sum_{\ell=0}^{\infty} \sum_{m=-\ell}^{\ell} F_{\ell m} Y_{\ell m}(\hat{\mathbf{s}}).$$

- The **spherical harmonic coefficients** are given by the usual projection onto the spherical harmonic basis functions:

$$F_{\ell m} = \int_{S^2} F(\hat{\mathbf{s}}) Y_{\ell m}^*(\hat{\mathbf{s}}) d\Omega(\hat{\mathbf{s}}),$$

where $d\Omega(\hat{\mathbf{s}}) = \sin \theta d\theta d\varphi$ is the usual rotation invariant measure on the sphere and $\hat{\mathbf{s}} = (\theta, \varphi) \in S^2$ denote spherical coordinates with colatitude $\theta \in [0, \pi]$ and longitude $\varphi \in [0, 2\pi)$.

- Useful **properties and relations**
 - Orthogonality

$$\int_{S^2} Y_{\ell m}(\hat{\mathbf{s}}) Y_{\ell' m'}^*(\hat{\mathbf{s}}) d\Omega(\hat{\mathbf{s}}) = \delta_{\ell\ell'} \delta_{mm'}$$

- Addition theorem

$$\sum_{m=-\ell}^{\ell} Y_{\ell m}(\hat{\mathbf{s}}) Y_{\ell m}^*(\hat{\mathbf{s}}') = \frac{2\ell + 1}{4\pi} P_{\ell}(\hat{\mathbf{s}} \cdot \hat{\mathbf{s}}')$$

- Jacobi-Anger expansion

$$e^{i\mathbf{x} \cdot \mathbf{y}} = \sum_{\ell=0}^{\infty} (2\ell + 1) i^{\ell} j_{\ell}(\|\mathbf{x}\| \|\mathbf{y}\|) P_{\ell}(\hat{\mathbf{x}} \cdot \hat{\mathbf{y}})$$

Rotations

- **Rotations on the sphere** \mathcal{R} characterised by the the rotation group $SO(3)$, which we parameterise in terms of the three Euler angles $\rho = (\alpha, \beta, \gamma) \in SO(3)$, where $\alpha \in [0, 2\pi)$, $\beta \in [0, \pi]$ and $\gamma \in [0, 2\pi)$.
- **Rotation of coordinate vector** performed by multiplication with 3×3 rotation matrix

$$\mathbf{R}(\rho) = \mathbf{R}_z(\alpha)\mathbf{R}_y(\beta)\mathbf{R}_z(\gamma) ,$$

where $\mathbf{R}_z(\vartheta)$ and $\mathbf{R}_y(\vartheta)$ are rotation matrices representing rotations by ϑ about the z and y axis respectively (adopt zyz Euler convention).

- **Rotation of function** on the sphere defined by

$$(\mathcal{R}(\rho)F)(\hat{s}) = F(\mathbf{R}^{-1}(\rho)\hat{s}) .$$

- Rotation of function on sphere may be performed more generally (*i.e.* pixelisation independent) and accurately through **harmonic space representation**. Harmonic coefficients of a rotated function are related to the coefficients of the original function by

$$(\mathcal{R}(\rho)F)_{\ell m} = \sum_{n=-\ell}^{\ell} D_{mn}^{\ell}(\rho) F_{\ell n} ,$$

where the Wigner D -functions $D_{mn}^{\ell}(\rho)$ provide the irreducible unitary representation of the rotation group $SO(3)$.

- For computational purposes, the Wigner functions may be decomposed as $D_{mn}^{\ell}(\alpha, \beta, \gamma) = e^{-im\alpha} d_{mn}^{\ell}(\beta) e^{-in\gamma}$; $d_{mn}^{\ell}(\beta)$ may then be computed rapidly using recursion formulae (Risbo [6]).

Rotations

- **Rotations on the sphere** \mathcal{R} characterised by the the rotation group $SO(3)$, which we parameterise in terms of the three Euler angles $\rho = (\alpha, \beta, \gamma) \in SO(3)$, where $\alpha \in [0, 2\pi)$, $\beta \in [0, \pi]$ and $\gamma \in [0, 2\pi)$.
- **Rotation of coordinate vector** performed by multiplication with 3×3 rotation matrix

$$\mathbf{R}(\rho) = \mathbf{R}_z(\alpha)\mathbf{R}_y(\beta)\mathbf{R}_z(\gamma) ,$$

where $\mathbf{R}_z(\vartheta)$ and $\mathbf{R}_y(\vartheta)$ are rotation matrices representing rotations by ϑ about the z and y axis respectively (adopt zyz Euler convention).

- **Rotation of function** on the sphere defined by

$$(\mathcal{R}(\rho)F)(\hat{s}) = F(\mathbf{R}^{-1}(\rho)\hat{s}) .$$

- Rotation of function on sphere may be performed more generally (*i.e.* pixelisation independent) and accurately through **harmonic space representation**. Harmonic coefficients of a rotated function are related to the coefficients of the original function by

$$(\mathcal{R}(\rho)F)_{\ell m} = \sum_{n=-\ell}^{\ell} D_{mn}^{\ell}(\rho) F_{\ell n} ,$$

where the Wigner D -functions $D_{mn}^{\ell}(\rho)$ provide the irreducible unitary representation of the rotation group $SO(3)$.

- For computational purposes, the Wigner functions may be decomposed as $D_{mn}^{\ell}(\alpha, \beta, \gamma) = e^{-im\alpha} d_{mn}^{\ell}(\beta) e^{-in\gamma}$; $d_{mn}^{\ell}(\beta)$ may then be computed rapidly using recursion formulae (Risbo [6]).

Coordinate systems

- The complex visibility measured by an interferometer is given by the **coordinate free definition**

$$\mathcal{V}(\mathbf{u}) = \int_{S^2} A(\boldsymbol{\sigma}) I(\boldsymbol{\sigma}) e^{-i2\pi \mathbf{u} \cdot \boldsymbol{\sigma}} d\Omega .$$

- In this coordinate free definition, $\boldsymbol{\sigma}$ is the representation of \hat{s} in a coordinate system centred on \hat{s}_0 . The translation $\boldsymbol{\sigma} = \hat{s} - \hat{s}_0$ represents the **transformation** between the global coordinate frame of \hat{s} and the local coordinate frame of $\boldsymbol{\sigma}$.
- In general, one can transform vectors between global coordinates and local coordinates relative to \hat{s}_0 , through a **rotation** by \hat{s}_0 .
- The rotation $\mathcal{R}_0 \equiv \mathcal{R}(\varphi_0, \theta_0, 0)$, where (θ_0, φ_0) are the spherical coordinates of \hat{s}_0 , transforms the local coordinate frame relative to \hat{s}_0 to the global coordinate frame of the celestial sky.
- Local coordinates are related to global coordinates by** $\hat{s}^l = \mathbf{R}_0^{-1} \hat{s}^n$, where \mathbf{R}_0 is the 3×3 rotation matrix corresponding to the rotation \mathcal{R}_0 .

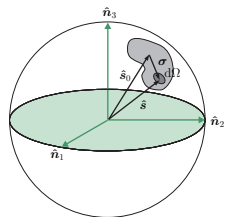


Figure: Geometry of observation of extended source.

Coordinate systems

- The complex visibility measured by an interferometer is given by the **coordinate free definition**

$$\mathcal{V}(\mathbf{u}) = \int_{S^2} A(\boldsymbol{\sigma}) I(\boldsymbol{\sigma}) e^{-i2\pi \mathbf{u} \cdot \boldsymbol{\sigma}} d\Omega .$$

- In this coordinate free definition, $\boldsymbol{\sigma}$ is the representation of $\hat{\mathbf{s}}$ in a coordinate system centred on $\hat{\mathbf{s}}_0$. The translation $\boldsymbol{\sigma} = \hat{\mathbf{s}} - \hat{\mathbf{s}}_0$ represents the **transformation** between the global coordinate frame of $\hat{\mathbf{s}}$ and the local coordinate frame of $\boldsymbol{\sigma}$.
- In general, one can transform vectors between global coordinates and local coordinates relative to $\hat{\mathbf{s}}_0$, through a **rotation** by $\hat{\mathbf{s}}_0$.
- The rotation $\mathcal{R}_0 \equiv \mathcal{R}(\varphi_0, \theta_0, 0)$, where (θ_0, φ_0) are the spherical coordinates of $\hat{\mathbf{s}}_0$, transforms the local coordinate frame relative to $\hat{\mathbf{s}}_0$ to the global coordinate frame of the celestial sky.
- Local coordinates are related to global coordinates by** $\hat{\mathbf{s}}^l = \mathbf{R}_0^{-1} \hat{\mathbf{s}}^n$, where \mathbf{R}_0 is the 3×3 rotation matrix corresponding to the rotation \mathcal{R}_0 .

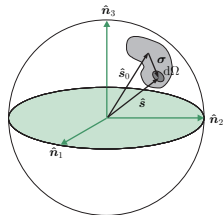


Figure: Geometry of observation of extended source.

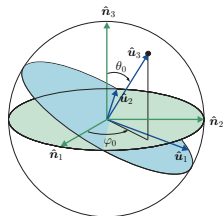


Figure: Rotation \mathcal{R}_0 mapping global coordinates of the celestial sky to local coordinates defined relative to the pointing direction $\hat{\mathbf{s}}_0$.

Coordinate systems

- Returning to the visibility function, we may now represent each function in its most **natural coordinate system**:
 - The beam function is most naturally represented in local coordinates relative to the pointing direction \hat{s}_0^n and is denoted by $A^1(\hat{s}^1)$.
 - The source intensity function is most naturally represented in global coordinates and is denoted by $I^n(\hat{s}^n)$.
- We may **convert function** F^n in global coordinates to a corresponding function F^1 in local coordinates through the rotation \mathcal{R}_0 :

$$F^n(\hat{s}^n) = F^n(\mathbf{R}_0\hat{s}^1) = (\mathcal{R}_0^{-1}F^n)(\hat{s}^1) = F^1(\hat{s}^1), \quad \text{i.e. } F^1 = \mathcal{R}_0^{-1}F^n.$$

- The **visibility integral** may then be written

$$\mathcal{V}(u) = \int_{S^2} A^1(\hat{s}^1) I^n(\hat{s}^n) e^{-i2\pi\mathbf{u}\cdot\hat{s}^1} d\Omega(\hat{s}^1),$$

or in local coordinates

$$\begin{aligned} \mathcal{V}(u) &= \int_{S^2} A^1(\hat{s}^1) (\mathcal{R}_0^{-1}I^n)(\hat{s}^1) e^{-i2\pi\mathbf{u}\cdot\hat{s}^1} d\Omega(\hat{s}^1) \\ &= \int_{S^2} A^1(\hat{s}^1) I^1(\hat{s}^1) e^{-i2\pi\mathbf{u}\cdot\hat{s}^1} d\Omega(\hat{s}^1). \end{aligned}$$

Coordinate systems

- Returning to the visibility function, we may now represent each function in its most **natural coordinate system**:
 - The beam function is most naturally represented in local coordinates relative to the pointing direction \hat{s}_0^n and is denoted by $A^1(\hat{s}^1)$.
 - The source intensity function is most naturally represented in global coordinates and is denoted by $I^n(\hat{s}^n)$.
- We may **convert function** F^n in global coordinates to a corresponding function F^1 in local coordinates through the rotation \mathcal{R}_0 :

$$F^n(\hat{s}^n) = F^n(\mathbf{R}_0\hat{s}^1) = (\mathcal{R}_0^{-1}F^n)(\hat{s}^1) = F^1(\hat{s}^1), \quad \text{i.e. } F^1 = \mathcal{R}_0^{-1}F^n.$$

- The **visibility integral** may then be written

$$\mathcal{V}(\mathbf{u}) = \int_{S^2} A^1(\hat{s}^1) I^n(\hat{s}^n) e^{-i2\pi\mathbf{u}\cdot\hat{s}^1} d\Omega(\hat{s}^1),$$

or in local coordinates

$$\begin{aligned} \mathcal{V}(\mathbf{u}) &= \int_{S^2} A^1(\hat{s}^1) (\mathcal{R}_0^{-1}I^n)(\hat{s}^1) e^{-i2\pi\mathbf{u}\cdot\hat{s}^1} d\Omega(\hat{s}^1) \\ &= \int_{S^2} A^1(\hat{s}^1) I^1(\hat{s}^1) e^{-i2\pi\mathbf{u}\cdot\hat{s}^1} d\Omega(\hat{s}^1). \end{aligned}$$

Computing visibilities

- **More general** and **accurate** to compute full-sky visibilities in harmonic space.
- Substituting the harmonic expansion of the beam-modulated source intensity function $(A^l \cdot I^l)(\hat{s}^l) = A^l(\hat{s}^l)I^l(\hat{s}^l)$, visibility integral becomes

$$\mathcal{V}(\mathbf{u}) = \sum_{\ell m} (A^l \cdot I^l)_{\ell m} \int_{S^2} e^{-i2\pi\mathbf{u} \cdot \hat{s}^l} Y_{\ell m}(\hat{s}^l) d\Omega(\hat{s}^l) .$$

- Using the addition theorem for spherical harmonics, the Jacobi-Anger expansion and the orthogonality of the spherical harmonics the above integral can be evaluated analytically:

$$\int_{S^2} e^{-i2\pi\mathbf{u} \cdot \hat{s}^l} Y_{\ell m}(\hat{s}^l) d\Omega(\hat{s}^l) = 4\pi (-i)^\ell j_\ell(2\pi\|\mathbf{u}\|) Y_{\ell m}(\hat{\mathbf{u}}) .$$

- The **harmonic representation of the full-sky visibility function** then reads:

Harmonic representation of visibility

$$\mathcal{V}(\mathbf{u}) = 4\pi \sum_{\ell m} (-i)^\ell j_\ell(2\pi\|\mathbf{u}\|) Y_{\ell m}(\hat{\mathbf{u}}) (A^l \cdot I^l)_{\ell m}$$

Image reconstruction

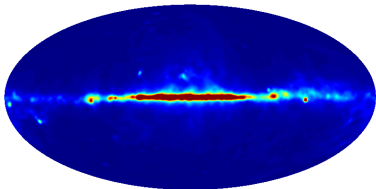
- Full-sky image reconstruction is **possible in theory**:

$$\int_{S^2} \mathcal{V}(\mathbf{u}) Y_{\ell m}^*(\hat{\mathbf{u}}) d\Omega(\hat{\mathbf{u}}) = 4\pi (-i)^\ell j_\ell(2\pi \|\mathbf{u}\|) (A^1 \cdot I^1)_{\ell m} .$$

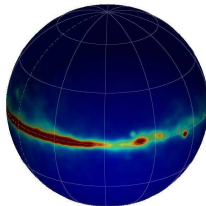
- But **not in practise** since would require full sampling of the visibility function in \mathbb{R}^3 .
- Instead use:
 - Standard Fourier transform approach for small patches.
 - w -projection (Cornwell *et al.* [2]) or faceting (*e.g.* Greisen [3]) approaches for wide fields of view.
- We consider only the forward problem of simulating visibilities in the full-sky setting and do not consider the reverse problem of image reconstruction any further.

Preliminary simulations

- **Challenging computational problem.**
- For a 50×50 pixel image of one square degree, require a harmonic band limit of $\ell_{\max} \simeq 13,000$.
- Solutions:
 - parallelise code;
 - fast methods such as wavelets (more to come on this).
- Present preliminary simulations here of **mock observations of synchrotron emission** (use synchrotron foreground map recovered from WMAP observations)



(a) Mollweide projection



(b) Globe

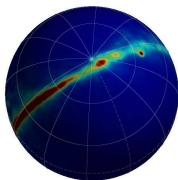
Figure: Full-sky synchrotron map observed by WMAP and smoothed with a Gaussian kernel of $\text{FWHM}_s = 1.7^\circ$.

Preliminary simulations

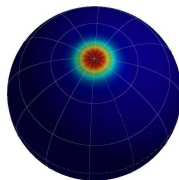
- **Low resolution simulations:** baseline limit of $u_{\max} = 30$; $\ell_{\max} \simeq 270$; reconstruct 20×20 image (corresponds to $\sim 20^\circ$ square patch).
- **Rotate to local coordinates** then compute visibilities for complete uv coverage, including full-sky contributions.
- Computations take **~ 5 minutes** on laptop (2.2GHz processor; 2GB RAM)
- Reconstructed image and tangent plane image **match reasonably closely**. Expected to differ slightly since:
 - full-sky contributions included when simulating visibilities but use Fourier transform to reconstruct image;
 - lose some high-frequency content due to low harmonic band-limit.

Preliminary simulations

- **Low resolution simulations**: baseline limit of $u_{\max} = 30$; $\ell_{\max} \simeq 270$; reconstruct 20×20 image (corresponds to $\sim 20^\circ$ square patch).
- **Rotate to local coordinates** then compute visibilities for complete uv coverage, including full-sky contributions.
- Computations take **~ 5 minutes** on laptop (2.2GHz processor; 2GB RAM)
- Reconstructed image and tangent plane image **match reasonably closely**. Expected to differ slightly since:
 - full-sky contributions included when simulating visibilities but use Fourier transform to reconstruct image;
 - lose some high-frequency content due to low harmonic band-limit.



(a) Synchrotron map

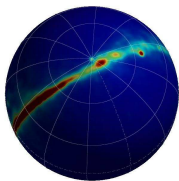


(b) Gaussian beam

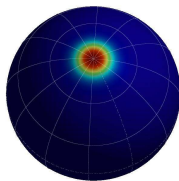
Figure: Full-sky synchrotron and beam maps in local coordinates.

Preliminary simulations

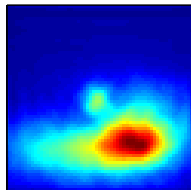
- **Low resolution simulations**: baseline limit of $u_{\max} = 30$; $\ell_{\max} \simeq 270$; reconstruct 20×20 image (corresponds to $\sim 20^\circ$ square patch).
- **Rotate to local coordinates** then compute visibilities for complete uv coverage, including full-sky contributions.
- Computations take **~ 5 minutes** on laptop (2.2GHz processor; 2GB RAM)
- Reconstructed image and tangent plane image **match reasonably closely**. Expected to differ slightly since:
 - full-sky contributions included when simulating visibilities but use Fourier transform to reconstruct image;
 - lose some high-frequency content due to low harmonic band-limit.



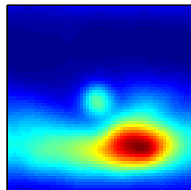
(a) Synchrotron map



(b) Gaussian beam



(a) Tangent plane



(b) Full-sky simulation

Figure: Full-sky synchrotron and beam maps in local coordinates.

Figure: Beam-modulated intensity images for a $\sim 20^\circ$ square patch.

Why wavelets?



Fourier (1807)



Haar (1909)

Morlet and Grossman (1981)

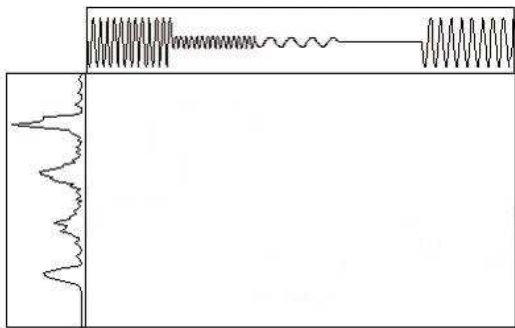


Figure: Fourier vs wavelet transform (image from <http://www.wavelet.org/tutorial/>)

Why wavelets?



Fourier (1807)



Haar (1909)

Morlet and Grossman (1981)

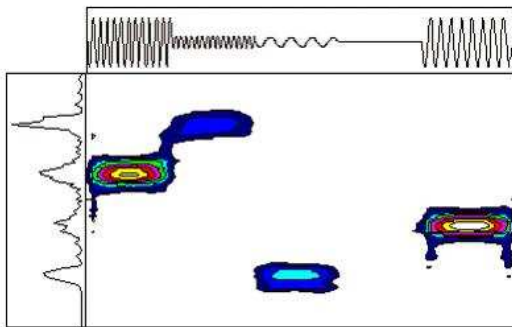


Figure: Fourier vs wavelet transform (image from <http://www.wavelet.org/tutorial/>)

Wavelets on the sphere

- **Continuous wavelets** on the sphere

Antoine & Vandergheynst [1], Wiaux *et al.* [9], McEwen *et al.* [5]

- Analysis:

$$\mathcal{W}_{\Psi}^f(a, \rho) = \int_{S^2} d\Omega(\hat{s}) f(\hat{s}) \Psi_{a, \rho}^*(\hat{s}) .$$

- Synthesis:

$$f(\hat{s}) = \int_{\text{SO}(3)} d\varrho(\rho) \int_0^{\infty} \frac{da}{a^3} \mathcal{W}_{\Psi}^f(a, \rho) [\mathcal{R}(\rho)\widehat{L}_{\Phi}\Psi_a](\hat{s}) ,$$

where $d\varrho(\rho) = \sin\beta d\alpha d\beta d\gamma$ is the invariant measure on the rotation group $\text{SO}(3)$ and \widehat{L}_{Φ} is a linear operator acting on the spherical harmonic coefficients of a function.

- **Discrete wavelets** on the sphere (multiresolution analysis)

Schroder & Sweldens [7], McEwen & Eysers [4], Starck *et al.* [8], Wiaux, McEwen *et al.* [10]

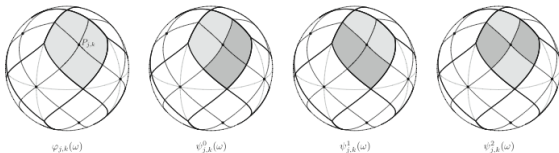


Figure: Haar scaling function and wavelets.

Wavelets on the sphere

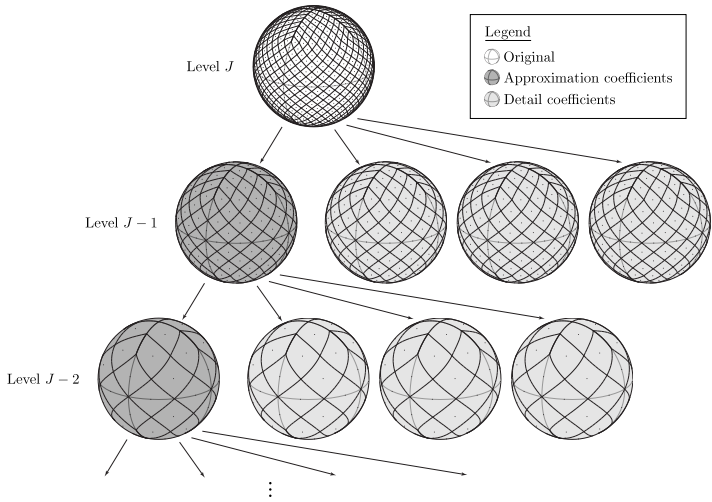


Figure: Haar multiresolution decomposition.

Fast wavelet methods

- Representing the beam-modulated intensity and the plane wave in an orthogonal wavelet basis on the sphere, with wavelets $\Psi_j(\hat{s}) \in L^2(S^2, d\Omega)$:

$$(A^1 \cdot I^1)(\hat{s}^1) = \sum_j (A^1 \cdot I^1)_j \Psi_j(\hat{s}^1);$$

$$e^{i2\pi \mathbf{u} \cdot \hat{s}^1} = \sum_k E_k(\mathbf{u}) \Psi_k(\hat{s}^1).$$

- Wavelet coefficients are given by the projection onto the wavelet basis functions:

$$(A^1 \cdot I^1)_j = \int_{S^2} (A^1 \cdot I^1)(\hat{s}^1) \Psi_j^*(\hat{s}^1) d\Omega(\hat{s}^1);$$

$$E_k(\mathbf{u}) = \int_{S^2} e^{i2\pi \mathbf{u} \cdot \hat{s}^1} \Psi_k^*(\hat{s}^1) d\Omega(\hat{s}^1).$$

- Substituting these expansions into the visibility integral we find

$$\mathcal{V}(\mathbf{u}) = \sum_j (A^1 \cdot I^1)_j E_j^*(\mathbf{u})$$

where we have **noted the orthogonality of the wavelet basis**.

- Naive **complexity** of computing visibility for given \mathbf{u} and \hat{s}_0 , is $\mathcal{O}(J)$, where J is the number of basis functions ($\mathcal{O}(J) \sim \mathcal{O}(\ell_{\max}^2)$ for the spherical harmonic basis).
- However, **effective complexity reduced substantially** by using a wavelet basis for which $(A^1 \cdot I^1)$ is sparse.

Summary & future work

- Derived **harmonic representation of visibility integral**, including full-sky contributions.
- Framework **allows extensions** to complicated beams that depend on pointing position (although not discussed in this talk).
- Performed very **preliminary simulations** to demonstrate and validate methodology.
- **Future directions:**
 - more realistic **high-resolution simulations** (parallelise implementation, incorporate extensions, incomplete uv coverage, evaluate effect of wide beam sidelobes);
 - fast wavelet methods to **reduce computational requirements**;
 - fast wavelet methods for wide field of view **image reconstruction?**

References

- [1] J.-P. Antoine and P. Vandergheynst.
Wavelets on the n -sphere and related manifolds.
J. Math. Phys., 39(8):3987–4008, 1998.
- [2] T. J. Cornwell, K. Golap, and S. Bhatnagar.
Wide Field Imaging: Fourier and Fresnel.
In *Astronomical Society of the Pacific Conference Series*, volume 345, pages 350–+, December 2005.
- [3] E. Greisen.
Wide field imaging in classical AIPS.
In *URSI General Assembly*, August 2002.
- [4] J. D. McEwen and D. M. Ewers.
Compression on the sphere.
In preparation, 2008.
- [5] J. D. McEwen, M. P. Hobson, and A. N. Lasenby.
A directional continuous wavelet transform on the sphere.
ArXiv, 2006.
- [6] T. Risbo.
Fourier transform summation of Legendre series and D -functions.
J. Geodesy, 70(7):383–396, 1996.
- [7] P. Schröder and W. Sweldens.
Spherical wavelets: efficiently representing functions on the sphere.
In *Computer Graphics Proceedings (SIGGRAPH '95)*, pages 161–172, 1995.
- [8] J.-L. Starck, Y. Moudden, P. Abrial, and M. Nguyen.
Wavelets, ridgelets and curvelets on the sphere.
Astron. & Astrophys., 446:1191–1204, February 2006.
- [9] Y. Wiaux, L. Jacques, and P. Vandergheynst.
Correspondence principle between spherical and Euclidean wavelets.
Astrophys. J., 632:15–28, 2005.
- [10] Y. Wiaux, J. D. McEwen, P. Vandergheynst, and O. Blanc.
Exact reconstruction with directional wavelets on the sphere.
Mon. Not. Roy. Astron. Soc., 2007.